MicroRNA-9 functions as a tumor suppressor and enhances radio-sensitivity in radio-resistant A549 cells by targeting neuropilin 1

KAI XIONG[1*], LI HONG SHAO[2*], HAI QIN ZHANG[2], LINLIN JIN[2], WEI WEI[2], ZHUO DONG[2], YUE QUAN ZHU[1], NING WU[3], SHUN ZI JIN[2] and LI XIANG XUE[1]

[1]Department of Radiation Oncology, Medical Research Center, Peking University Third Hospital, Beijing 100191; [2]Key Laboratory of Radiobiology, Ministry of Health, Jilin University, Changchun, Jilin 130021; [3]Department of Radiation Oncology, China-Japan Union Hospital of Jilin University, Changchun, Jilin 130033, P.R. China

Received January 10, 2017; Accepted November 10, 2017

DOI: 10.3892/ol.2017.7705

Abstract. Radiotherapy is commonly used to treat lung cancer but may not kill all cancer cells, which may be attributed to the radiotherapy resistance that often occurs in non-small cell lung cancer (NSCLC). At present, the molecular mechanism of radio-resistance remains unclear. Neuropilin 1 (NRP1), a co-receptor for vascular endothelial growth factor (VEGF), was demonstrated to be associated with radio-resistance of NSCLC cells via the VEGF-phosphoinositide 3-kinase-nuclear factor-κB pathway in our previous study. It was hypothesized that certain microRNAs (miRs) may serve crucial functions in radio-sensitivity by regulating NRP1. Bioinformatics predicted that NRP1 was a potential target of miR-9, and this was validated by luciferase reporter assays. Functionally, miR-9-transfected A549 cells exhibited a decreased proliferation rate, increased apoptosis rate and attenuated migratory and invasive abilities. Additionally, a high expression of miR-9 also significantly enhanced the radio-sensitivity of A549 cells *in vitro* and *in vivo*. These data improve understanding of the mechanisms of cell radio-resistance, and suggest that miR-9 may be a molecular target for the prediction of radio-sensitivity in NSCLC.

Correspondence to: Professor Li Xiang Xue, Department of Radiation Oncology, Medical Research Center, Peking University Third Hospital, 49 Huayuan North Road, Haidian, Beijing 100191, P.R. China
E-mail: lixiangxue@hsc.pku.edu.cn

Professor Shun Zi Jin, Key Laboratory of Radiobiology, Ministry of Health, Jilin University, 1163 Xinmin Street, Changchun, Jilin 130021, P.R. China
E-mail: jinsz@jlu.edu.cn

*Contributed equally

Key words: ionizing radiation, microRNA-9, non-small cell lung cancer, radio-sensitivity

Introduction

Lung cancer is a global health problem with poor clinical outcomes. According to the survey of Mayo Clinic in 2005, non-small cell lung cancer (NSCLC) accounts for more than 80% of 5,628 patients with primary lung cancer out of all lung cancer cases, and the majority of patients with NSCLC are diagnosed at the advanced stage (1-3). Radiation therapy is regarded as the primary treatment strategy for NSCLC. However, radio-resistance is a key issue limiting its effectiveness (4). Therefore, screening for effective molecular radiosensitizers is urgently required to provide personalized therapy and improve patient survival.

MicroRNAs (miRs; miRNAs) are endogenous non-coding RNAs that function as regulators of gene expression by targeting mRNA degradation or inhibiting their translation (5). Over the previous decade, a number of studies have demonstrated that the altered expression of miRs has been associated with different types of cancer (6), including lung cancer (7). In addition, studies have also suggested that there is an association between certain miRs and radiotherapy (8,9). The function of miR-9 in cancer cells has been considered to be controversial since it serves as a tumor suppressor in melanoma (10) and as a metastasis-promoter in breast cancer (11). Reduced expression of miR-9 is considered to be a marker of poor prognosis in cervical cancer (12) and acute lymphoblastic leukemia (13). However, the function of miR-9 in NSCLC pathogenesis, and the molecular mechanisms by which miR-9 exerts its functions and modulates the malignant phenotypes of NSCLC cells have not been fully determined.

Neuropilin 1 (NRP1) is a transmembrane glycoprotein with large extracellular regions that is extensively expressed in endothelial cells and a variety of tumor cells (14). NRP1 serves a crucial function in tumorigenesis and radio-resistance. Brieger *et al* (15) identified that the addition of recombinant vascular endothelial growth factor VEGF-121 and VEGF-165 to squamous carcinoma cells increased resistance to radiation-induced cell death by targeting NRP1 receptors. Glinka *et al* (16) demonstrated that the overexpression of NRP1 decreased the apoptosis rate of glioma cells induced by radiation. In our previous study, NRP1

was highly expressed in the radio-resistant NSCLC A549 cell line, and short hairpin RNA-mediated NRP1 inhibition significantly enhanced radio-sensitivity (17). However, the mechanism by which NRP1 is regulated by certain miRs to exert its functions remains unclear.

The present study demonstrated that miR-9 served a tumor suppressor function in, and enhanced the radio-sensitivity of, NSCLC cells by regulating NRP1. These data will provide novel insights for understanding the mechanisms of NSCLC pathogenesis, and present a potential biomarker in evaluating the effectiveness of radio-therapy treatment.

Materials and methods

Cell lines and treatment. A549 cells were cultured in Dulbecco's modified Eagle medium (DMEM; Gibco; Thermo Fisher Scientific, Inc., Waltham, MA, USA). All media were supplemented with 10% fetal bovine serum (FBS; HyClone; GE Healthcare, Chicago, IL, USA), 100 U/ml penicillin and 100 μg/ml streptomycin (Beijing Solarbio Science & Technology Co., Ltd., Beijing, China) in a humid incubator with 5% CO_2. Cells were harvested using 0.25% trypsin (Beijing Solarbio Science & Technology Co., Ltd., Beijing, China) and 0.03% EDTA solution at 37˚C for 5-10 min. Media were replaced 2-3 times per week.

A549 cells (Type Culture Collection of the Chinese Academy of Sciences, Shanghai, China) were cultured in Dulbecco's modified Eagle's medium (Gibco, Thermo Fisher Scientific, Inc., Waltham, MA, USA) supplemented with 10% (vol/vol) fetal bovine serum (HyClone, GE Healthcare) and 1% penicillin-streptomycin. A549 cells were transfected with 100 nM miR-9 mimic (Sense 5'-UCUUUGGUUAUCUAG CUGUAUGATT-3', Anti-sense 5'-AUAAAGCUAGAUAAC CGAAAGUTT-3) or negative control (NC; Sense 5'-UUC UCCGAACGUGUCACGUTT-3', Anti-sense 5'-ACGUGA CACGUUCGGAGAATT-3') RNA (GenePharma, Shanghai, China) using Lipofectamine® 2000 (Invitrogen; Thermo Fisher Scientific, Inc., Waltham, MA, USA) were sham-irradiated or exposed to irradiation (IR). Subsequent experimentation was performed 24 h after transfection.

Experimental animals. A total of 24 male 6-week-old Balb/c athymic nude mice (Beijing HFK Bioscience Co., Ltd., Beijing, China), weighing 19-20 g were used in this study. Mice were maintained in a specific pathogen free environment, with a 12 h light/dark cycle at 20-25˚C and a humidity of 40-70%, sterilized food and water were freely available. Mice were subcutaneously injected in the right flank with $1x10^6$ cells in 0.1 ml PBS. Once the tumors had formed, caliper measurements were performed daily and tumor volume (V) was calculated using the formula: $V=width^2xlength/2$. When tumors volume reached ~100 mm^3, the mice were randomly divided into four groups (control, miR-9, IR and miR-9+IR group; n=6), and the miR-9 and miR-9+IR groups received intratumoral injection of miR-9 plasmids along with the DNA transfection reagent (Entranster™-*in vivo*, Engreen Biosystem Co., Ltd., Beijing, China) once weekly. For each injection, 15 μg miRNA were mixed with 15 μl Entranster™-*in vivo*. The IR and miR-9+IR group were exposed to 20 Gy at the tumor site. The mice were euthanatized 15 days following IR, or if a humane endpoint was reached; defined as a loss of more than 15% of body mass, a tumor volume greater than 1.2 cm^3, severe fever, vomiting or skin problems (wounds or signs of inflammation) or inability to ambulate or rise for food and water. Following euthanasia, the tumor mass and volume were recorded, and tumor volumes did not exceed 219 mm^3. The dissected tumors were collected and prepared for subsequent analyses. All animal experiments were performed in accordance with the institutional guidelines of Jilin University (Changchun, China) for the Care and Use of Laboratory Animals, and this board approved the study protocol was.

Irradiation. A549 cells were sham-irradiated or exposed to IR at a dose rate of 1.0 Gy/min (220 kV; 18 mA) by an X-ray generator (Model X-RAD320, Precision X-ray, North Branford, CT, USA). The male 6-week-old Balb/c athymic nude mice were exposed to a single 20 Gy dose of X rays at a dose rate of 1.55 Gy/min.

RNA isolation and quantitative polymerase chain reaction (RT-qPCR). Total RNA was extracted from A549 cells using TRIzol® reagent (Invitrogen; Thermo Fisher Scientific, Inc., Waltham, MA, USA) and reverse transcribed to generate cDNA (PrimeScript RT-PCR kit; Takara Bio, Inc., Otsu, Japan) according to the manufacturer's protocol. The primer sequences are as follows: NPR1 forward, CCCCAAACCACT GATAACTCG, reverse, AGACACCATACCCAACATTCC; GAPDH forward, ACATCGCTCAGACACCATG, reverse, TGTAGTTGAGGTCAATGAAGGG (Sangon Biotech Co., Ltd., Shanghai, China). The Thermocycling conditions were as follows: 95˚C for 5 min, 40 cycles of 95˚C for 10 sec follows by 60˚C for 30 sec. U6 small nuclear RNA and GAPDH were used as internal controls for miR-9 and NRP1, respectively. All samples were normalized to the internal controls and fold changes were calculated through relative quantification ($2^{-\Delta\Delta Cq}$) (18).

miRNA conserved target sites prediction in 3' UTR of NRP1. The TargetScan predictions (http://www.targetscan.org/vert_71/) were used to identify the putative miRNA target sites in 3' UTRs of *NRP1* gene. The *NRP1* gene symbol and human species were retrieved from the database. The 3' UTR of *NRP1* transcript ENST00000374875.1 was selected to analyze the potential binding site of miRNAs.

Plasmid construction and luciferase reporter assays. Gaussian luciferase and alkaline phosphatase activities were measured by luminescence in conditioned medium (DMEM; HyClone; GE Healthcare) without antibiotics and 10% FBS (HyClone; GE Healthcare) 48 h after transfection, as previously described (19). A 2,600 bp fragment of DNA from the NRP1 3' untranslated region (3'UTR) of A549 cells was amplified by PCR using Q5® High-Fidelity DNA Polymerase (M0491) from New England BioLabs, Inc. (Ipswich, MA, USA). The primer sequences used were as follows: Forward, ATGAACGGT ACCAGGCAGACAGAGATGAAAAGACA, reverse, GAA CTTCTCGAGTCAGGTGTGGGATATTTTATGAAAATG. Thermocycling conditions were 95˚C for 3 min, followed by 35 cycles of 95˚C for 15 sec, 58˚C for 30 sec, 72˚C for 2 min 30 sec, 35 cycles, and one cycle of 72˚C for 10 min. DNA was then cloned into the pEZX-MT05 vector (GeneCopoeia,

Inc., Rockville, MD, USA). The vector was named wild-type (wt) 3'UTR. Site-directed mutagenesis of the miR-9 binding site in the NRP1 3'UTR was performed using the GeneTailor Site-Directed Mutagenesis System (Invitrogen; Thermo Fisher Scientific, Inc.) and the construct was named mutant (mt) 3'UTR. A549 cells were transfected with 100 ng wt/mt 3'UTR vectors and 100 nM miR-9 mimic/anti-miR-9/NC, using Lipofectamine® 2000 (Invitrogen; Thermo Fisher Scientific, Inc.). Following transfection for 48 h, the activity of Gaussia luciferase and secreted alkaline phosphatase were examined using the Secrete-Pair Dual Luminescence Assay kit (GeneCopoeia, Inc., Rockville, MD, USA). Gaussian luciferase activity was normalized to alkaline phosphatase activity. Normalized luciferase activity of treatment group was compared with that of control group.

Western blot analysis. A total of 48 h after radiation exposure, media was removed from the A549 cells, which were then washed twice with ice-cold PBS. Lysis was performed using cell lysis buffer (Beyotime Institute of Biotechnology, Haimen, China), and cell lysates were collected by scraping the plates prior to centrifugation at 10,000 x g at 4˚C for 5 min. Proteins were quantified using a bicinchoninic acid assay kit according to the manufacturers protocol (Applygen Technologies Inc., Beijing, China). A total of 30 μg protein, denatured in gel loading buffer (Applygen Technologies Inc., Beijing, China), was loaded per well and separated using SDS-PAGE electrophoresis (5% stacking gel and 10% separating gel) at 100 V voltage until bromophenol blue runs out of separating gel, and then transferred onto polyvinylidene fluoride membranes (Bio-Rad Laboratories, Inc., Hercules, CA, USA). The membranes were blocked in 5% skimmed milk at room temperature for 1 h, prior to incubation at 4˚C overnight with the designated primary antibodies (rabbit anti-Neuropilin 1 (Abcam, Cambridge, UK; cat. no., ab81321), rabbit anti-phospho-p38 MAPK (CST Biological Reagents Co., Ltd., Shanghai, China; cat. no., 9215), rabbit anti-total-p38 MAPK (Sigma-Aldrich; Merck KGaA, Darmstadt, Germany; cat. no., M0800), rabbit anti-pERK1/2 (T202/Y204) (CST Biological Reagents Co., cat. no., 4370), mouse anti-ERK1/2 (CST Biological Reagents Co., cat. no., 9107), rabbit anti-pAKT (S473; CST Biological Reagents Co., cat. no., 4060), mouse anti-AKT (CST Biological Reagents Co. cat. no., 2966), rabbit PI3 Kinase p110α (C73F8; CST Biological Reagents Co., cat. no., 4249) and mouse anti-GAPDH (Santa Cruz Biotechnology, Inc., Dallas, TX, USA; cat. no., sc-47724). All antibodies were used at a dilution of 1:1,000. Membranes were then incubated with the corresponding horseradish peroxidase-conjugated secondary antibodies (goat anti-rabbit IgG; Beyotime Institute of Biotechnology) for 2 h at room temperature. Densitometry was performed using ImageJ (version 1.50i; National Institutes of Health, Bethesda, MD, USA).

Cell viability assay. A total of $5x10^3$ A549 cells were seeded into 96-well plates and transfected with miR-9 mimics or control RNA. Following IR, the cells were cultured in DMEM (Hyclone; GE Healthcare, Chicago, IL, USA) with 10% FBS (HyClone; GE Healthcare) at 37˚C for 0, 24 and 48 h. The effect of miR-9 on cell growth and viability was determined by MTT assay (Cell Growth Determination kit; Sigma-Aldrich; Merck KGaA, Darmstadt, Germany) according to the manufacturer's instructions, DMSO was used to dissolve the crystals, and the optical density was measured at 570 nm.

Cell-cycle analysis and Annexin V-fluorescein isothiocyanate (FITC) apoptosis detection assay. For cell-cycle analysis, $1x10^6$ cells transfected with miRNAs or control RNA were cultured in complete DMEM (Hyclone; GE Healthcare) at 37˚C in triplicate in 6-well plates. At 48 h post-transfection, cells were exposed to 10 Gy IR. The cell-cycle distribution was analyzed by 0.05 mg/ml propidium iodide staining (37˚C for 30 min) and flow cytometry (BD Biosciences, Franklin Lakes, NJ, USA). The cells were stained for 20 min at room temperature using the Annexin V-FITC Apoptosis Detection kit I (BD Biosciences) according to the manufacturer's protocol. The data obtained from this assay was analyzed using Modfit software (version 3.3; Verity House Software, Topsham, ME, USA).

Colony formation assays. Transfected and control A549 cells were plated into 6-well plates at specific cell densities (200 cells for 0 Gy, 500 cells for 2 Gy, 1,000 cells for 4 Gy, 3,000 cells for 6 Gy and 5,000 cells for 8 Gy) and received 0, 2, 4, 6 or 8 Gy X-ray 24 h subsequent to seeding, and were then cultured in DMEM (Hyclone; GE Healthcare) at 37˚C for 7-14 days to allow colonies to grow. The cells were then rinsed 3 times with PBS, fixed in 100% methanol (at room temperature for 20 min), and stained with Giemsa stain (0.04%) for 30 min at room temperature. The number of the colonies containing at least 50 cells was counted using a light microscope at magnification, x40. The surviving fraction was calculated as the number of colonies counted/(the number of cells seeded x plating efficiency). Experiments were performed in triplicate and repeated three times.

In vitro migration and invasion assays. For the transwell migration assays, $2.5x10^4$ A549 cells were plated in the top chamber on non-coated membrane (24-well insert; Corning, NY, USA). For the invasion assays, $5x10^4$ A549 cells were plated in the top chamber on Matrigel®-coated membranes (24-well insert; BD Biosciences). The cells were plated in DMEM (Hyclone; GE Healthcare) without serum, or supplemented 10% FBS (HyClone; GE Healthcare) was used as the chemoattractant in the lower chamber. The cells were then incubated for 12 h at 37˚C. Cells remaining on the upper side of the filter membrane were removed with PBS-rinsed cotton swabs. The filters were then fixed in 100% ethanol for 20 min at room temperature, and stained with 0.1% crystal violet for 20 min at room temperature. The stained cells were counted under a light microscope (magnification, x40). The average count was calculated in 6 random fields of view. Experiments were performed in triplicate and repeated three times.

Statistical analysis. Statistical analysis was performed using SPSS 18.0 (SPSS, Inc., Chicago, IL, USA). The results from three independent experiments are presented as mean ± standard deviation. Differences between the control and experimental groups were analyzed using one-way analysis of variance, followed by between group comparisons performed using the Student-Newman-Keuls test. $P<0.05$ was considered to indicate a statistically significant difference.

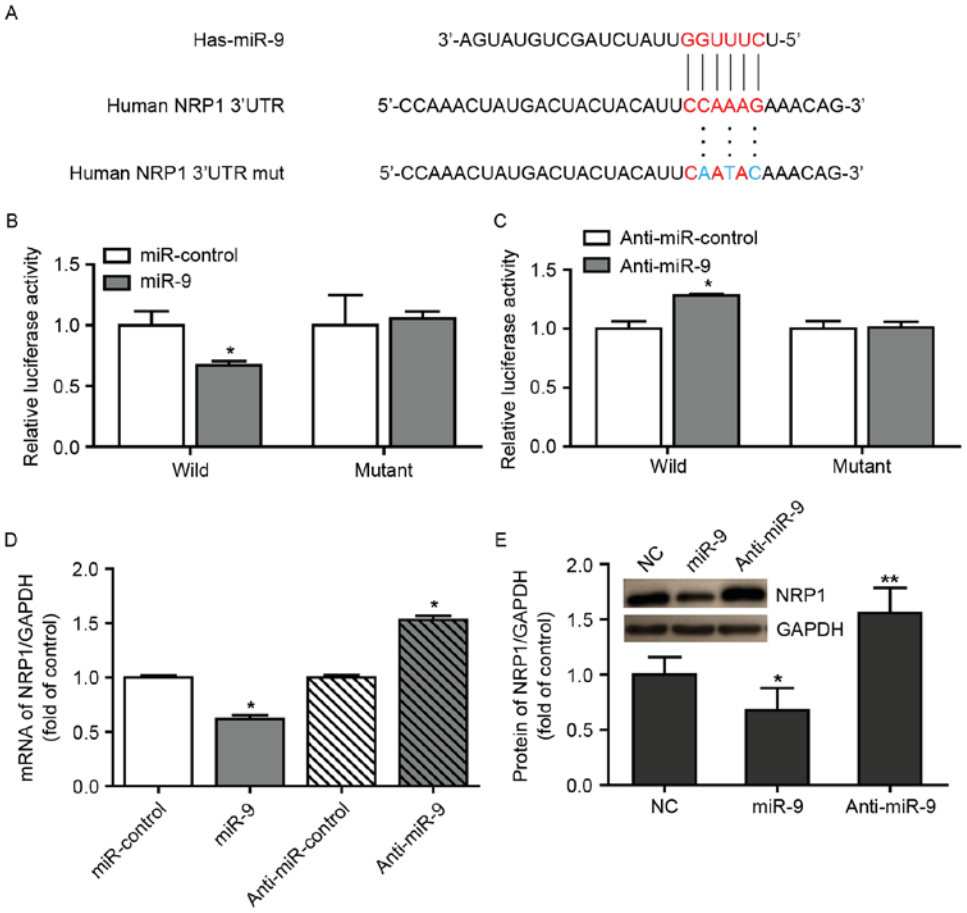

Figure 1. miR-9 regulates NRP1 expression in A549 cells. (A) Putative miR-9 binding site in NRP1. The potential complementary residues are highlighted in red, and site-directed mutagenesis of the miR-9 binding site are indicated in blue. (B) Co-transfection with miR-9 mimics and wt 3'UTR NRP1 constructs decreased the luciferase activity compared with the miR-control. The effect was diminished when the mutations of putative binding site were introduced. (C) Co-transfection with anti-miR-9 and wt 3'UTR NRP1 constructs increased the luciferase activity compared with anti-miR-control. The effect was diminished when the mutations of putative binding site were introduced. (D) Reverse transcription quantitative polymerase chain reaction analysis demonstrated that the NRP1 mRNA expression was downregulated in A549 cells transfected with miR-9 mimics compared with miR-control, but this expression was upregulated in cells transfected with anti-miR-9 compared with anti-miR-control. (E) Western blot analysis of NRP1 in lysates of A549 cells co-transfected with miR-9, miR-control or anti-miR-9. Representative immunoblot (upper panel) and densitometric analysis (lower panel) from three separate experiments. *P<0.05 and **P<0.01 vs. control. Has, *Homo sapiens*; miR, microRNA; NRP1, Neuropilin 1; UTR, untranslated region; NC, negative control; wt, wild type.

Results

NRP1 is a direct target of miR-9 in A549 cells. In our previous study, it had been demonstrated that a high expression of NRP1 was correlated with the growth, survival and radio-resistance of NSCLC cells via the VEGF-PI3K-NF-κB pathway (17). We hypothesized that certain miRNAs may be involved in these biological processes through regulating NRP1 expression. In view of this consideration, the present study used the TargetScan algorithm to determine the potential miRNAs that may bind to the 3'UTR of NRP1 and it was identified that NRP1 possessed a conserved miR-9 binding site within its 3'UTR in the majority of species examined (Fig. 1A). A luciferase reporter assay was additionally performed to identify the ability of miR-9 to bind to the 3'UTR of NRP1 mRNA. Notably, co-transfecting the miR-9 mimics with the luciferase-linked NRP1 wild-type 3'UTR construct downregulated luciferase activity, whereas co-transfection with the mutated 3'UTR construct did not (Fig. 1B). In addition, inhibition of endogenous miR-9 expression in cells transduced with anti-miR-9 resulted in increased luciferase activity from the wild-type construct, but had no effect on the mutated NRP1 3'UTR (Fig. 1C). These data suggest that miR-9 regulated the expression of NRP1 mRNA (Fig. 1D) and protein (Fig. 1E) in A549 cells.

miR-9 serves a tumor suppressor role in A549 cells in vitro and in vivo. The expression of NRP1 was detected in 5 NSCLC cell lines including H358, H460, H1299, A549 and SK-MES-1 in a previous study (17), and it was identified that the A549 cell line demonstrated the highest expression of NRP1 and the strongest radio-resistance. In addition, the tumors formed from NRP1-inhibited A549 cells grew at a decreased rate compared with those from normal A549 cells (17). Therefore, A549 cells were selected as the primary cell line. Whether miR-9 overexpression functioned similarly to NRP1 inhibition was examined. miR-9 mimics were transiently transfected into A549 cells for functional analysis. A significant decrease in cell viability at 24 h and a more marked decrease at 48 h was observed compared with the control (Fig. 2A). Concurrently, a significant increase in apoptosis was detected with miR-9 treatment vs. the control (Fig. 2B). Cell cycle assays indicated that transfection with

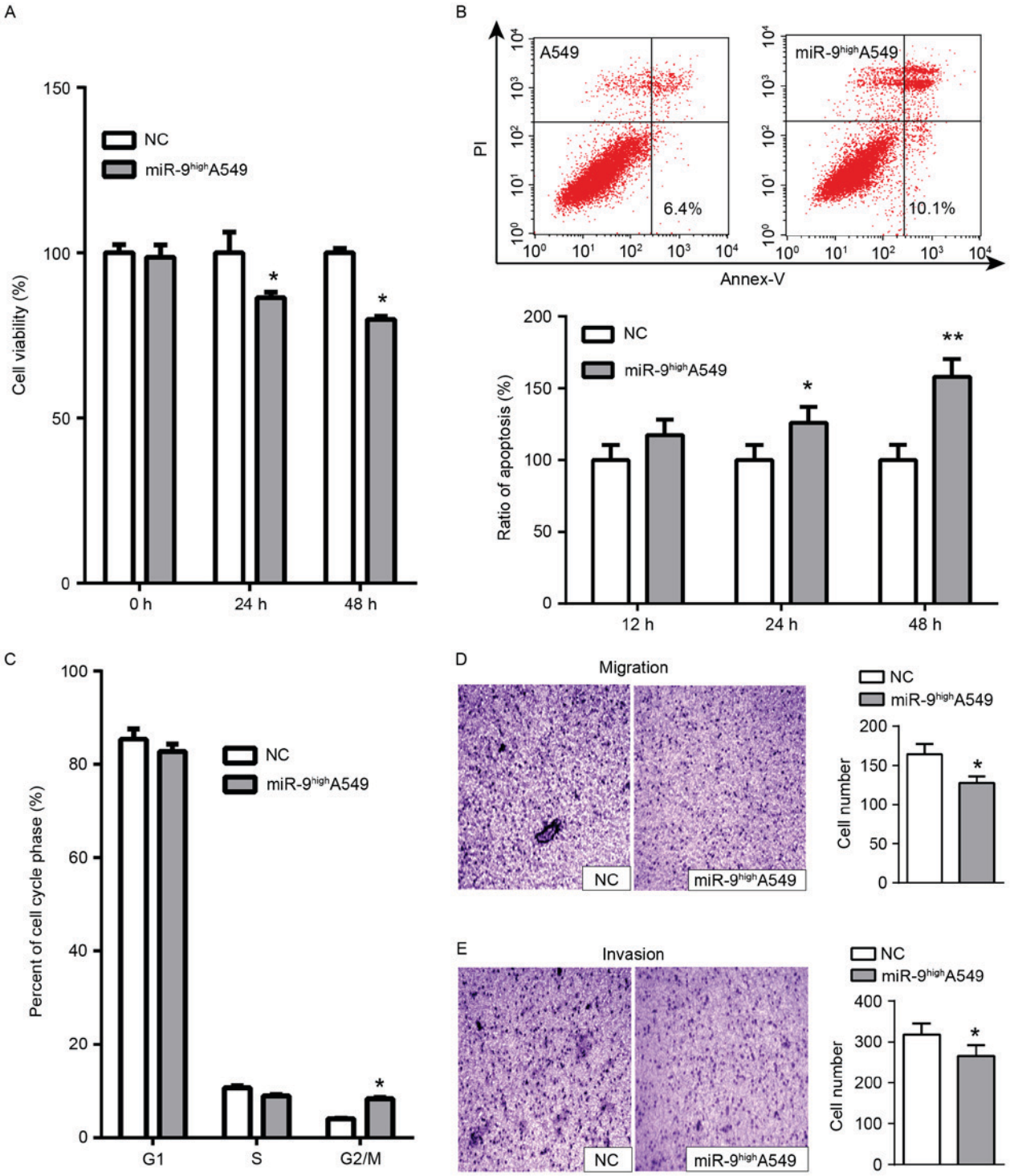

Figure 2. Effects of miR-9 overexpression on non-small cell lung cancer cells *in vitro*. (A) MTT assay demonstrated that miR-9 overexpression led to a marked reduction in cell viability. (B) Representative images of flow cytometry analysis of apoptotic cells by Annexin V assay at 48 h post-transfection of miR-9 mimics (upper panel). Histograms indicate the A549 cell apoptosis ratio at 12, 24 and 48 h post-transfection of miR-9 mimics (lower panel). (C) Flow cytometry demonstrates that miR-9 arrested the cell cycle progression in phase G2/M. The (D) migratory and (E) invasive capacities of A549 cells transfected with miR-9 mimics were reduced. Data are presented as mean ± standard deviation of three independent experiments. *P<0.05 and **P<0.01 vs. control. NC, negative control; miR, microRNA; PI, propidium iodide.

miR-9 mimics arrested cell cycle progression in the G2/M phase at 48 h (Fig. 2C). In addition, we measured the migratory and invasive abilities of A549 cells via transwell migration and Matrigel® invasion assays. The results indicated that the number of migratory (Fig. 2D) and invasive cells (Fig. 2E) decreased following transfection with miR-9 mimics compared with untreated A549 cells. Furthermore, the tumor formation assay in nude mice demonstrated that the growth of tumors formed from miR-9-treated A549 cells was delayed compared with the normal control group (Fig. 3C). Overall, these results indicated that miR-9 functioned as a tumor suppressor in A549 cells by inhibiting cell

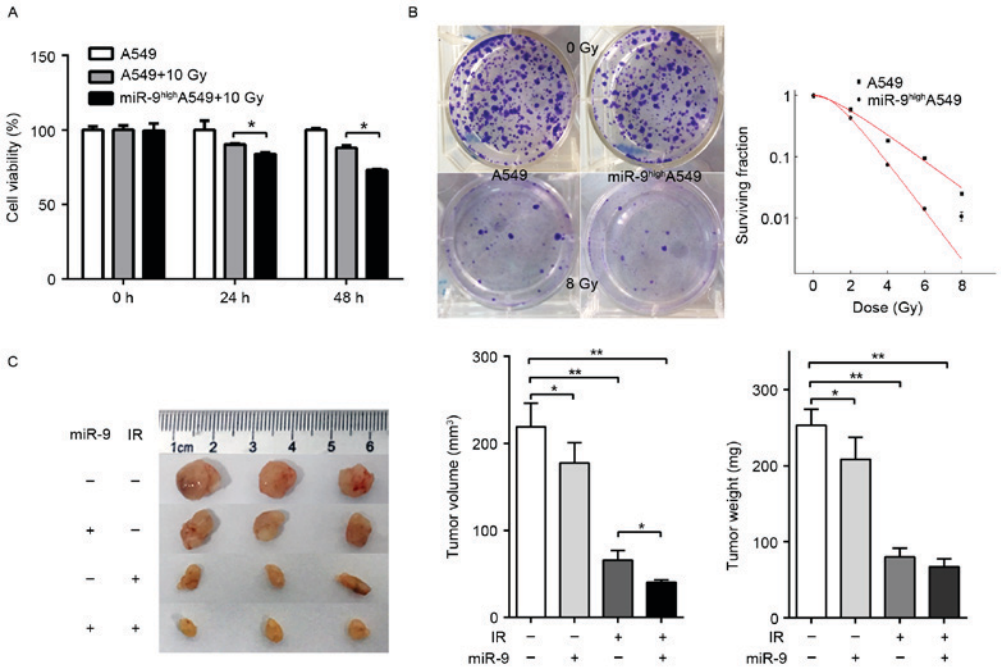

Figure 3. Effects of miR-9 overexpression on radio-sensitivity of A549 cells *in vitro* and *in vivo*. (A) MTT assay demonstrated that miR-9 overexpression led to a marked reduction in cell viability 24 and 48 h post-IR. (B) Clonogenic survival of transfected or un-transfected A549 cells. Compared with the control cells, miR-9-transfected cells demonstrated significantly lower clonogenic survival rates. (C) At 15 days following IR, the mice were euthanized, and the tumor volume and mass were calculated. The volume and weight of tumors from the miR-9- and IR-treated groups were more significantly decreased compared with that of other groups. Data are presented as the mean ± standard deviation of three independent experiments. *P<0.05 and **P<0.01 vs. control. IR, irradiation; miR, microRNA.

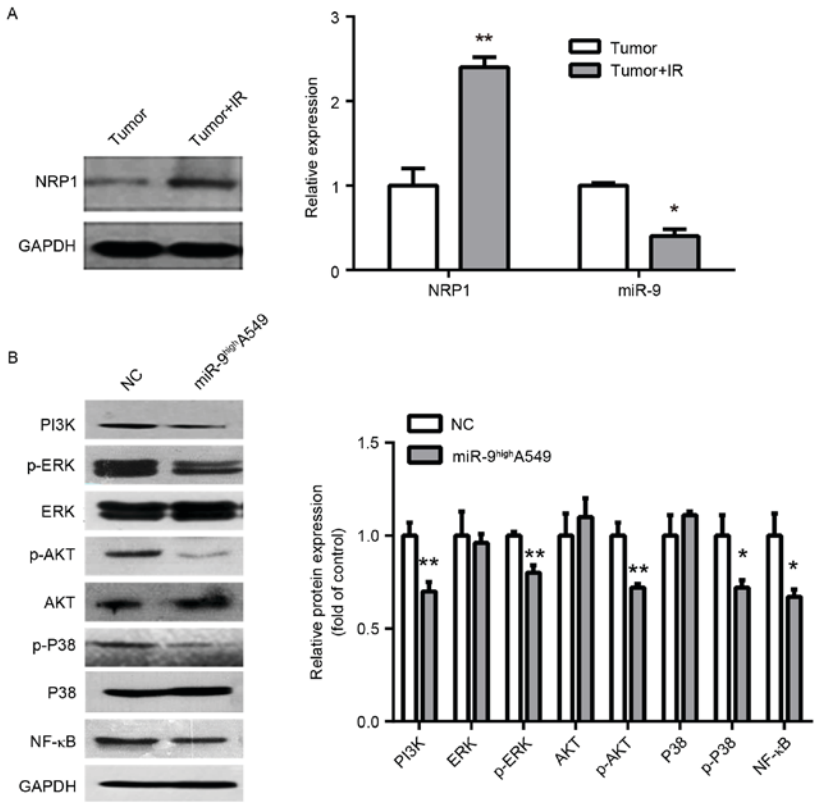

Figure 4. Exploration of the mechanism of radio-sensitivity. (A) Western blot analysis of NRP1 with IR and non-IR treated tumors from nude mice (left panel). Histograms demonstrate densitometric analysis of NRP1/GAPDH protein expression by western blotting and miR-9 expression by reverse transcription quantitative polymerase chain reaction from three separate experiments (right panel). IR upregulated NRP1 protein expression and downregulated miR-9 expression. (B) Representative immunoblots (left panel) of A549 cells infected with miR-NC or miR-9 indicated downregulation of PI3K/AKT, MAPK/ERK, NF-κB signaling protein by miR-9. Right panel is densitometric analysis of NRP1/GAPDH from three separate experiments. *P<0.05 and **P<0.01 vs. control. NRP, Neuropilin; miR, microRNA; p, phosphorylated; PI3k, phosphoinositide 3-kinase; ERK, extracellular signal-related kinase; AKT, protein kinase B; P38, P38 mitogen-activated protein kinase; NF-κB, nuclear factor κB; NC, negative control.

proliferation, promoting apoptosis and attenuating migratory and invasive capacities.

miR-9 overexpression enhances the radio-sensitivity of A549 cells in vitro and in vivo. It had been demonstrated previously that knockdown of endogenous NRP1 enhanced the radio-sensitivity of A549 cells (17). Combined with the results of the present study, we hypothesized that miR-9 was also able to effect the radio-sensitivity of A549 cells. A549 cells were transfected with or without miR-9 mimics and the effect upon IR was observed. The viability of cells transfected with miR-9 mimics was significantly decreased at 24 h, and even greater at 48 h compared with the normal control (Fig. 3A). Colony assays indicated that the survival fraction of A549 cells in the miR-9-transfected group was decreased compared with that in the miR-NC group upon IR with 0, 2, 4, 6 or 8 Gy (Fig. 3B). These data suggested that the overexpression of miR-9 may significantly enhance the *in vitro* radio-sensitivity of NSCLC cells. Next, the nude mouse subcutaneous tumor model was constructed. The mice were randomly divided into four groups (control, miR-9, IR and miR-9+IR group) and the corresponding experimental treatment was administered. The results indicated that the growth of the tumors treated with miR-9 and IR were significantly delayed compared with other groups (Fig. 3C), which suggested that miR-9 overexpression combined with radiotherapy may induce a stronger *in vivo* anti-tumor effect compared with radiotherapy alone.

Exploration on the mechanism of radio-sensitivity regulated by miR-9. The expression of NRP1 and miR-9 in IR- and non-IR-treated tumors from the nude mice were additionally examined. The NRP1 expression was significantly upregulated, while the miR-9 was markedly downregulated, which indicates a marked correlation with radiosensitivity (Fig. 4A). As a non-tyrosine kinase receptor, NRP1 may moderately increase PI3K and phosphorylation of ERK P38 MAPK, ERK1/2, protein kinase B (Akt) and NF-κB to promote tumor cell proliferation and metastasis, and inhibit apoptosis and enhance radio-resistance (17,20). Therefore, as NRP1 is a downstream target of miR-9, miR-9 may also downregulate PI3K and the phosphorylation of P38 MAPK, ERK1/2, Akt and NF-κB. Consequently, it was identified that the overexpression of miR-9 inhibited PI3K and phosphorylation of NF-κB, P38 MAPK, ERK1/2 and Akt, but the relative expression of total protein was not significantly altered (Fig. 4B). Therefore, one of the mechanisms of miR-9-mediated radio-sensitivity may function by regulating PI3K and the phosphorylation of NF-κB, ERK1/2, P38 MAPK and Akt via NRP1.

Discussion

miRs serve a crucial function in controlling proliferation, differentiation and tumorigenesis. A previous study demonstrated the downregulation of miR-9 in gastric, colon and ovarian cancer, and miR-9 upregulation in human breast cancer, brain tumors and biliary tract cancer associated with the controversial functions (21). miR-9 exhibits tumor-suppressive activity in human gastric cancer (22) and colorectal cancer (23), whilst it serves an oncogenic role in bladder cancer (24), osteosarcoma (25) and mixed lineage leukemia-rearranged leukemia (26). These conflicting results are also reflected in studies on the same types of tumors, such as ovarian cancer (27,28) and NSCLC (21,29), in which miR-9 has exhibited tumorigenesis-associated and anti-tumor activities in different studies. The reasons for these contradicting conclusions may be due to the heterogeneity of the tumors and the different materials, such as cell lines, used. In the present study, it was identified that miR-9 may inhibit the proliferation, invasion and migration in A549 cells, which possessed marked radio-resistance compared with other NSCLC cell lines. In addition, it was associated with the high expression of NRP1 (17). In the present study, it was demonstrated that miR-9 directly downregulated expression of NRP1 by binding to its 3'UTR and enhanced the radio-sensitivity of A549 cells.

To understand the clinicopathological significance of miR-9, the effect of miR-9 overexpression in A549 lung cancer cells was examined. The results indicated that miR-9 overexpression significantly decreased the viability of A549 cells and arrested cell cycle progression at the G2/M phase. As it has been established that cells in the G2/M phase are sensitive to IR, with sensitivity decreasing as cells proceed from G1 to S phase (30), the results from the flow cytometry analysis suggested that upregulation of miR-9 may enhance A549 cell radio-sensitivity by disrupting the G2/M phase of the cell cycle. In addition, the overexpression of miR-9 increased the cell apoptosis rate and inhibited cell migration and invasion compared with the transfected group. These results were consistent with those observed in NRP1 knockdown cells in our previous study (17), indicating that miR-9 serves a role of tumor suppressor by targeting NRP1 in A549 cells. In fact, NRP1 is an oncogenic promoter that is expressed in a wide variety of human tumor cell lines, and it has been demonstrated that NRP1 may enhance the binding of VEGF to vascular endothelial growth factor receptor 2 (VEGFR2), which resulted in promoting VEGF165-mediated tumor angiogenesis, cell migration and tumorigenicity (31).

It was also suggested that NRP1 may increase the resistance of tumor cells to radiotherapy (17,32). Therefore, we hypothesized that miR-9 may be also involved in the regulation of radiosensitivity. It was identified that miR-9 overexpression significantly inhibited the viability and colony-forming ability of A549 cells following IR, which demonstrated that miR-9 enhanced the radio-sensitivity of this cell line *in vitro*. Furthermore, a nude mouse subcutaneous tumor model was constructed to analyze the effect of miR-9 to radiotherapy. The results indicated that miR-9 overexpression, combined with IR, exerted a more marked anti-tumor effect compared with IR alone. All these data suggest that miR-9 enhanced the radio-sensitivity *in vitro* and *in vivo*.

The intrinsic tumor radio-resistance relies on cell survival and apoptosis, cell cycle and DNA repair pathways (33). A total of 4 classical signal transduction pathways, including PI3K/AKT, MAPK/ERK, NF-κB and transforming growth factor-β, were involved in the regulation of tumor radiation response, which may be activated either upon radiation exposure or through the phosphorylation of receptor tyrosine kinase such as EGFR and Insulin-like growth factor 1 receptor (34). The results of the present study revealed that treatment with IR inhibited miR-9 expression, and correspondingly increased NRP1 expression in the tumors formed from A549 cells. The

upregulated NRP1 expression increased the rate interaction between VEGFR2 and NRP1 and enhanced radio-resistance by the activated VEGFR2-PI3K-NF-κB pathway (17,20). It implied that increasing radio-sensitivity by upregulating miR9, which targets NRP1, may be a potential treatment strategy. Compared with the control group in the present study, the expression levels of PI3K, NF-κB, phosphorylated (p)ERK, pAkt and pP38 were all altered following the overexpression miR-9, indicating that miR-9 may inhibit multiple signaling pathways to enhance radio-sensitivity. These results may offer insights for the improved understanding of the whole network regulating radio-resistance, and may assist additional improvements in the radiotherapy treatment strategy for NSCLC.

Acknowledgements

The present study was supported by the National Natural Science Foundation of China (grant no. 81573085, 81672091, 81541142, 81371890 and 81201737) and Beijing Natural Science Foundation (grant no. 7172232). An abstract for this study was published following its acceptance for a poster presentation at the Annual Meeting-American Society for Radiation Oncology 24-27 September 2017, San Diego, CA, USA (International Journal of Radiation Oncology 99: E628, 2017).

References

1. Spiro SG and Silvestri GA: One hundred years of lung cancer. Am J Respir Crit Care Med 172: 523-529, 2005.
2. Parkin DM, Bray F, Ferlay J and Pisani P: Global cancer statistics, 2002 CA Cancer J Clin 55: 74-108, 2005.
3. Yang P, Allen MS, Aubry MC, Wampfler JA, Marks RS, Edell ES, Thibodeau S, Adjei AA, Jett J and Deschamps C: Clinical features of 5,628 primary lung cancer patients: Experience at Mayo Clinic from 1997 to 2003. Chest 128: 452-462, 2005.
4. Siegel R, Naishadham D and Jemal A: Cancer statistics, 2012. CA Cancer J Clin 62: 10-29, 2012.
5. Lee RC, Feinbaum RL and Ambros V: The C. elegans heterochronic gene lin-4 encodes small RNAs with antisense complementarity to lin-14. Cell 75: 843-854, 1993.
6. Calin GA and Croce CM: MicroRNA signatures in human cancers. Nat Rev Cancer 6: 857-866, 2006.
7. Ortholan C, Puissegur MP, Ilie M, Barbry P, Mari B and Hofman P: MicroRNAs and lung cancer: New oncogenes and tumor suppressors, new prognostic factors and potential therapeutic targets. Curr Med Chem 16: 1047-1061, 2009.
8. Salim H, Akbar NS, Zong D, Vaculova AH, Lewensohn R, Moshfegh A, Viktorsson K and Zhivotovsky B: miRNA-214 modulates radiotherapy response of non-small cell lung cancer cells through regulation of p38MAPK, apoptosis and senescence. Br J Cancer 107: 1361-1373, 2012.
9. Oh JS, Kim JJ, Byun JY and Kim IA: Lin28-let7 modulates radiosensitivity of human cancer cells with activation of K-Ras. Int J Radiat Oncol Biol Phys 76: 5-8, 2010.
10. Liu S, Kumar SM, Lu H, Liu A, Yang R, Pushparajan A, Guo W and Xu X: MicroRNA-9 up-regulates E-cadherin through inhibition of NF-κB1-Snail1 pathway in melanoma. J Pathol 226: 61-72, 2012.
11. Ma L, Young J, Prabhala H, Pan E, Mestdagh P, Muth D, Teruya-Feldstein J, Reinhardt F, Onder TT, Valastyan S, *et al*: miR-9, a MYC/MYCN-activated microRNA, regulates E-cadherin and cancer metastasis. Nat Cell Biol 12: 247-256, 2010.
12. Hu X, Schwarz JK, Lewis JS Jr, Huettner PC, Rader JS, Deasy JO, Grigsby PW and Wang X: A microRNA expression signature for cervical cancer prognosis. Cancer Res 70: 1441-1448, 2010.
13. Rodriguez-Otero P, Román-Gómez J, Vilas-Zornoza A, José-Eneriz ES, Martín-Palanco V, Rifón J, Torres A, Calasanz MJ, Agirre X and Prosper F: Deregulation of FGFR1 and CDK6 oncogenic pathways in acute lymphoblastic leukaemia harbouring epigenetic modifications of the MIR9 family. Br J Haematol 155: 73-83, 2011.
14. Wild JR, Staton CA, Chapple K and Corfe BM: Neuropilins: Expression and roles in the epithelium. Int J Exp Pathol 93: 81-103, 2012.
15. Brieger J, Schroeder P, Gosepath J and Mann WJ: VEGF-subtype specific protection of SCC and HUVECs from radiation induced cell death. Int J Mol Med 15: 145-151, 2005.
16. Glinka Y, Mohammed N, Subramaniam V, Jothy S and Prud'homme GJ: Neuropilin-1 is expressed by breast cancer stem-like cells and is linked to NF-κB activation and tumor sphere formation. Biochem Biophys Res Commun 425: 775-780, 2012.
17. Dong JC, Gao H, Zuo SY, Zhang HQ, Zhao G, Sun SL, Han HL, Jin LL, Shao LH, Wei W and Jin SZ: Neuropilin 1 expression correlates with the Radio-resistance of human non-small-cell lung cancer cells. J Cell Mol Med 19: 2286-2295, 2015.
18. Livak KJ and Schmittgen TD: Analysis of relative gene expression data using real-time quantitative PCR and the 2(-Delta Delta C(T)) method. Methods 25: 402-408, 2001.
19. Hershkovitz-Rokah O, Modai S, Pasmanik-Chor M, Toren A, Shomron N, Raanani P, Shpilberg O and Granot G: MiR-30e induces apoptosis and sensitizes K562 cells to imatinib treatment via regulation of the BCR-ABL protein. Cancer Lett 356: 597-605, 2015.
20. Hong TM, Chen YL, Wu YY, Yuan A, Chao YC, Chung YC, Wu MH, Yang SC, Pan SH, Shih JY, *et al*: Targeting neuropilin 1 as an antitumor strategy in lung cancer. Clin Cancer Res 13: 4759-4768, 2007.
21. Xu T, Liu X, Han L, Shen H, Liu L and Shu Y: Up-regulation of miR-9 expression as a poor prognostic biomarker in patients with non-small cell lung cancer. Clin Transl Oncol 16: 469-475, 2014.
22. Wan HY, Guo LM, Liu T, Liu M, Li X and Tang H: Regulation of the transcription factor NF-kappaB1 by microRNA-9 in human gastric adenocarcinoma. Mol Cancer 9: 16, 2010.
23. Zhu M, Xu Y, Ge M, Gui Z and Yan F: Regulation of UHRF1 by microRNA-9 modulates colorectal cancer cell proliferation and apoptosis. Cancer Sci 106: 833-839, 2015.
24. Wang H, Zhang W, Zuo Y, Ding M, Ke C, Yan R, Zhan H, Liu J and Wang J: miR-9 promotes cell proliferation and inhibits apoptosis by targeting LASS2 in bladder cancer. Tumour Biol 36: 9631-9640, 2015.
25. Zhu SW, Li JP, Ma XL, Ma JX, Yang Y, Chen Y and Liu W: miR-9 modulates osteosarcoma cell growth by targeting the GCIP tumor suppressor. Asian Pac J Cancer Prev 16: 4509-4513, 2015.
26. Chen P, Price C, Li Z, Li Y, Cao D, Wiley A, He C, Gurbuxani S, Kunjamma RB, Huang H, *et al*: miR-9 is an essential oncogenic microRNA specifically overexpressed in mixed lineage leukemia-rearranged leukemia. Proc Natl Acad Sci USA 110: 11511-11516, 2013.
27. Zhao HM, Wei W, Sun YH, Gao JH, Wang Q and Zheng JH: MicroRNA-9 promotes tumorigenesis and mediates sensitivity to cisplatin in primary epithelial ovarian cancer cells. Tumour Biol 36: 6867-6873, 2015.
28. Guo LM, Pu Y, Han Z, Liu T, Li YX, Liu M, Li X and Tang H: MicroRNA-9 inhibits ovarian cancer cell growth through regulation of NF-kappaB1. FEBS J 276: 5537-5546, 2009.
29. Wang J, Yang B, Han L, Li X, Tao H, Zhang S and Hu Y: Demethylation of miR-9-3 and miR-193a genes suppresses proliferation and promotes apoptosis in non-small cell lung cancer cell lines. Cell Physiol Biochem 32: 1707-1719, 2013.
30. Pawlik TM and Keyomarsi K: Role of cell cycle in mediating sensitivity to radiotherapy. Int J Radiat Oncol Biol Phys 59: 928-942, 2004.
31. Murga M, Fernandez-Capetillo O and Tosato G: Neuropilin-1 regulates attachment in human endothelial cells independently of vascular endothelial growth factor receptor-2. Blood 105: 1992-1999, 2005.
32. Kawakami T, Tokunaga T, Hatanaka H, Kijima H, Yamazaki H, Abe Y, Osamura Y, Inoue H, Ueyama Y and Nakamura M: Neuropilin 1 and neuropilin 2 co-expression is significantly correlated with increased vascularity and poor prognosis in nonsmall cell lung carcinoma. Cancer 95: 2196-2201, 2002.
33. Yahyanejad S, Theys J and Vooijs M: Targeting Notch to overcome radiation resistance. Oncotarget 7: 7610-7628, 2016.
34. Zhao L, Lu X and Cao Y: MicroRNA and signal transduction pathways in tumor radiation response. Cell Signal 25: 1625-1634, 2013.